Plant Soil
https://doi.org/10.1007/s11104-024-06696-6

RESEARCH ARTICLE

Reduced belowground allocation of freshly assimilated C contributes to negative plant-soil feedback in successive winter wheat rotations

Nikolaos Kaloterakis · Sirgit Kummer · Samuel Le Gall · Youri Rothfuss · Rüdiger Reichel · Nicolas Brüggemann

Received: 13 October 2023 / Accepted: 24 April 2024

Abstract

Aims Successive winter wheat (WW) rotations are associated with yield reduction, often attributed to the unfavorable soil microbes that persist in the soil through plant residues. How rotational positions of WW affect the allocation of freshly assimilated carbon (C), an energy source for soil microbes, above and belowground remains largely unknown.

Methods A $^{13}CO_2$ pulse labeling rhizotron experiment was conducted in the greenhouse to study freshly fixed C allocation patterns. WW was grown in soil after oilseed rape (W1), after one season of WW (W2), and after three successive seasons of WW (W4). We used an automatic manifold system to measure excess ^{13}C of soil respiration at six depths and five different dates. Excess ^{13}C was also measured in dissolved organic C (DOC), microbial and plant biomass pools.

Results There was a strong yield decline in successive WW rotations accompanied by distinct changes in root growth. Higher excess ^{13}C of soil respiration was measured in W1 compared to W4, especially in the topsoil during at later growth stages. Higher excess ^{13}C of the DOC and the microbial biomass was also traced in W1 and W4 compared to W2. Less ^{13}C was taken up by successive WW rotations.

Conclusions Our study demonstrates a mechanism through which the rotational position of WW affects the allocation of freshly assimilated C above and belowground. WW after oilseed rape sustains belowground allocation of freshly assimilated C for a longer time than successively grown WW and incorporates more of this C to its biomass.

Keywords Carbon allocation · ^{13}C pulse labeling · Gross rhizodeposition · Root-derived carbon · Rotational position · Winter wheat

Introduction

Winter wheat (WW) is the most cultivated staple crop in the world and a staple food for billions of people worldwide, contributing significantly to many national economies (Shewry and Hey 2015; Enghiad et al. 2017). Following a linear increase for many decades, annual WW yield growth is currently stagnating, not meeting the forecasted global demand (Calderini and Slafer 1998; Ray et al. 2013; Moore

Supplementary Information The online version contains supplementary material available at https://doi.org/10.1007/s11104-024-06696-6.

Responsible editor: Jens-Arne Subke.

N. Kaloterakis (✉) · S. Kummer · S. Le Gall · Y. Rothfuss · R. Reichel · N. Brüggemann
Institute of Bio- and Geosciences, Forschungszentrum Jülich GmbH, Agrosphere (IBG-3), 52428 Jülich, Germany
e-mail: nikoskaloter@gmail.com; n.kaloterakis@fz-juelich.de

Published online: 06 May 2024

and Lobell 2015; Schauberger et al. 2018). A 2.4% increase in crop yields is required annually to achieve food security by 2050. For WW, the current 0.9% annual yield growth is markedly lagging behind this target (Ray et al. 2013; Crespo-Herrera et al. 2018). Brisson et al. (2010) attributed this observation to agronomic (cereal rotations with more oilseed rape and fewer legumes, lower N fertilization), climatic (drought stress), and political causes (agricultural policies), while genetic progress did not appear to be an underlying cause.

Plant community diversity and succession has been associated with distinct changes in the abiotic and biotic parameters of the soil exerting positive or negative plant-soil feedbacks (PSF, van der Putten et al. 2013; de Vries et al. 2023). Among those, changes in nutrient input as well as contrasting quantity and quality (C: N ratio) of plant litter induce significant changes in the microbial community diversity and composition (Bennett and Klironomos 2019; Thakur et al. 2021; De Long et al. 2023). Linking the PSF theory to arable farming, the beneficial effect of a non-cereal pre-crop on WW productivity has been well established and yet it is estimated that up to 40% of the global WW cultivation is grown successively (Angus et al. 2015; Yin et al. 2022). This trend is expected to continue in the future due to the focus of agrochemical and breeding companies on the staple crops such as WW (Hegewald et al. 2018). This practice is associated with a high risk of soil-borne pathogens and specifically the necrotrophic fungus *Gaeumannomyces graminis* var. *tritici* (Ggt), which causes early root senescence, rotting, and yield decline (Cook 2003; Kwak and Weller 2013). Ggt can persist in the soil as a saprotroph after WW, has been harvested and its severity increases with increasing frequency of WW self-succession (Palma-Guerrero et al. 2021). However, the soil legacy of wheat monocropping is not limited to Ggt as this has been observed in years without obvious Ggt symptoms, suggesting that other soil microbes might contribute to the observed effect (Donn et al. 2015; Arnhold et al. 2023). The inclusion of oilseed rape in crop rotations has been widely appreciated for its importance to soil structure, suppression of WW pathogens, high post-harvest residual N and the production of secondary metabolites i.e., isothiocyanate (Sieling et al. 2005; Weiser et al. 2017; Hegewald et al. 2018; Hansen et al. 2019). Therefore, the soil legacy of the WW preceding crop to the following WW can be expected to exert major control over the productivity of WW.

Plants allocate photosynthetic C belowground for root growth and maintenance, as indicated by biomass buildup and root respiration (Jones et al. 2009). A part of that C is exuded from the roots into the rhizosphere, which is a hotspot for microbe-root interactions. This process is termed rhizodeposition and, in combination with root litter and dissolved organic C (DOC), it constitutes a readily available energy source for soil microorganisms (Kuzyakov and Domanski 2000; Loeppmann et al. 2019). Rhizodeposition may provide positive or negative feedback for plant nutrient acquisition as indicated by accelerated or decelerated nutrient mineralization by rhizosphere microorganisms (Cheng and Kuzyakov 2005; Tian et al. 2013; Meier et al. 2017). It has been established that the rhizodeposition-to-root biomass ratio shows very small variation, meaning that factors affecting root growth are also expected to affect C allocation belowground (Pausch et al. 2013; Heinemann et al. 2023). The combination of heterotrophic microbial respiration of rhizodeposits with autotrophic root respiration constitutes the root-derived CO_2 and can be used to estimate the fate of freshly assimilated C in plants (Loeppmann et al. 2019; Henneron et al. 2022). Whether successively grown WW invests more C belowground to stimulate root growth, root biomass and/or microbial activity, or whether it invests less C belowground due to negative soil legacy of the preceding crop, remains unknown.

^{13}C labeling of plants is a common and valuable approach to distinguish and quantify the rhizodeposited C from native soil organic C (SOC). It allows for the investigation of C allocation patterns throughout the soil and within the different plant parts (Bahn et al. 2013). In addition, recording the time lag between ^{13}C fixation and rhizodeposition belowground provides important information regarding the C use within plants as well as the availability of photosynthates to soil microorganisms (Brüggemann et al. 2011). Studying C partitioning to the different plant parts and to rhizodeposition has great potential to improve our understanding of C allocation patterns in high-input agricultural systems that are governed by intense microbial interactions and often abiotic stress factors. C allocation dynamics vary depending on plant species, plant genotype, plant

developmental stage (higher exudation during earlier growth stages), biotic and abiotic factors (Pausch and Kuzyakov 2018; Williams and de Vries 2020; Chai and Schachtman 2022). In WW, higher exudation for increased nutrient uptake is observed from early growth until flowering with a decreasing trend thereafter until full maturity (Sun et al. 2018). At this late developmental stage, C is transported to the head during starch synthesis of the grains (Sun et al. 2019). Rhizodeposition moderates microbial-plant competition by the provision of labile C and the resulting enhanced nutrient cycling when the nutritional demands of the plants are maximal (Hernández-Calderón et al. 2018; Mohan et al. 2020).

In light of no Ggt-resistant WW cultivars (Palma-Guerrero et al. 2021), the projected unfavorable climatic conditions for WW cultivation both at European and global scale (Senapati et al. 2021; Zhu et al. 2022) and the premature status of the Ggt-specific biocontrol research (Osborne et al. 2018; Zhao et al. 2023), there is an urgent need to decipher the mechanisms by which the rotational positions of WW influences its productivity. Here, we investigated how different rotational positions of WW influence the allocation of freshly assimilated C in above- and belowground plant parts and its subsequent translocation to the rhizosphere of WW. We hypothesized that WW self-succession would result in:

I. a limited assimilate supply to the root system and the associated soil microorganisms in successively grown WW due to negative soil legacy feedback and its associated decreased plant and root growth.
II. reduced storage of freshly assimilated C in aboveground plant parts and especially sink organs (grains) due to reduced root performance.

To test these hypotheses, a greenhouse rhizotron experiment was set up with three contrasting rotational positions of WW. The plants were pulse-labeled with enriched $^{13}CO_2$, and the allocation of freshly assimilated C was traced in the top- and subsoil over a 25-day period, spanning from flowering until grain filling stage.

Materials and methods

Experimental design

Soil was collected in September 2020 from the experimental farm Hohenschulen (54°19′05″N, 9°58′38″E), Faculty of Agricultural and Nutritional Sciences, Christian-Albrechts-University of Kiel, Germany. The crop rotation that is implemented in the experimental farm is: faba beans - oats - oil seed rape - WW -WW -WW. The soil is a Cambic Luvisol of sandy loam texture (44% sand, 35% silt and 21% clay; Sieling et al. 2005) with no carbonates. Soil was collected from the topsoil (0–30 cm) and subsoil (30–50 cm), from plots after oilseed rape cultivation (W1), first (W2) and third wheat (W4) after oilseed rape cultivation, and sieved to 2 mm. Hereafter, they are referred to as rotational positions. The initial soil properties are summarized in Table 1. The WW cultivar "Nordkap" was sown on the plots where the soil was collected. They were fertilized with nitrogen (240 kg N ha^{-1} split into three doses of 80 kg N ha^{-1} and applied at BBCH 25, 30/31 and 50/51; Zadoks et al. 1974). The residues of the preceding crop were not removed from the soil, and the field was not plowed before sampling. Note that the presence of Ggt experimental plots is well documented (Sieling et al. 2005).

We conducted a greenhouse rhizotron experiment (May 10, 2021 to November 12, 2021), using newly designed rhizotrons with a height of 100 cm, width of 35 cm and inner thickness of 2.5 cm (Reichel et al. 2022). The greenhouse was located on the campus of Forschungszentrum Jülich, Germany. The experiment was organized in a full factorial and completely randomized design, consisting of the three rotational positions W1, W2 and W4 with four replicates each, resulting in 12 experimental units (rhizotrons). The rhizotrons were rotated randomly on a weekly basis. For the online isotopic measurements that are described below, we took measurements of W1 and W4 but not W2, as W1 and W4 comprised the most extreme rotational positions and showed the most pronounced differences in their root growth. Three replicates from W1 and W4 were used for the isotopic measurements. Those rhizotrons were equipped with gas-permeable tubing (KM-PPMF_O-2020-KF-0201, Katmaj Filtration, Poland; 35 cm length, 0.155 cm wall thickness, 0.55 cm i.d., 0.86 cm o.d., 0.2 µm pore size) and polyethylene/aluminum tubing (Synflex®

Table 1 Initial soil NO_3^-, NH_4^+, plant-available P_{CAL}, K_{CAL}, sulfate (SO_4^{2-}), magnesium (Mg), C:N ratio, pH, DOC, microbial biomass carbon (C_{mic}), microbial biomass nitrogen (N_{mic}) and C_{mic}:N_{mic} for the soil from the different rotational positions. The soil for these analyses was collected from the 0–30 cm soil depth. Data are mean ± S.E. ($n = 3$ for rotational position). Different lowercase letters in each column denote significant differences between the rotational positions at $p \leq 0.05$ using Bonferroni correction for multiple comparisons. ANOVA main effects of rotational position are indicated as follows: ns = not significant; * $p \leq 0.05$; ** $p \leq 0.01$; *** $p \leq 0.001$

Soil parameter	Unit	Rotational position			ANOVA
		W1	W2	W4	
NO_3^-	mg N kg^{-1}	3.89 ± 0.03a	3.38 ± 0.11b	3.09 ± 0.00b	***
NH_4^+	mg N kg^{-1}	0.11 ± 0.01	0.14 ± 0.02	0.18 ± 0.03	**ns**
P_{CAL}	mg kg^{-1}	19.3 ± 0.1a	16.1 ± 0.2b	18.4 ± 1.0ab	*
K_{CAL}	mg kg^{-1}	51.3 ± 0.8a	27.8 ± 0.7c	35.4 ± 0.2b	***
SO_4^{2-}	mg kg^{-1}	5.3 ± 0.3a	3.5 ± 0.2b	2.9 ± 0.0b	***
Mg	mg kg^{-1}	75.2 ± 1.7	76.8 ± 1.4	84.6 ± 3.0	**ns**
soil C: N		9.74 ± 0.02	9.63 ± 0.03	9.68 ± 0.08	**ns**
pH		6.73 ± 0.00	6.76 ± 0.01	6.75 ± 0.01	**ns**
DOC	mg kg^{-1}	29.5 ± 0.3a	22.6 ± 0.7b	29.0 ± 0.2a	***
C_{mic}	mg kg^{-1}	57.0 ± 2.0b	41.2 ± 3.4c	75.3 ± 1.2a	***
N_{mic}	mg kg^{-1}	8.2 ± 0.2a	4.3 ± 0.5b	9.3 ± 0.2a	***
C_{mic}:N_{mic}		7.0 ± 0.3b	9.6 ± 0.3a	8.1 ± 0.3b	**

1300, ¼" o.d., Eaton, Bonn, Germany). The gas-permeable tubing was positioned horizontally in the soil at six depths (5, 15, 25, 35, 65 and 85 cm) and connected to the sampling system with the Synflex® tubing. The tubing was sealed until it was used for the isotopic measurements. In this way, air exchange between the inner volume of the gas-permeable tubing and the ambient air in the greenhouse could be avoided and water vapor loss minimized.

All rhizotrons were kept inclined at 45° to facilitate root growth along the lower side of the rhizotrons. Bulk density was adjusted to 1.45 g cm^{-3} using topsoil (collected from 0 to 30 cm) for the first 30 cm and subsoil (collected from 30 to 50 cm) for the following 70 cm. Deionized water was added to reach 70% water-holding capacity (WHC, 215 g H_2O soil kg^{-1}) at the onset of the experiment. Thereafter, soil moisture was readjusted gravimetrically every 2–3 days to 70% WHC to ensure well-watered conditions. WW seeds (cultivar "Nordkap") were germinated on petri dishes with sterile filter paper for 24 h in the dark at 20 °C. Subsequently, one germinated seed was sown into each rhizotron. Each plant was fertilized with 0.78 g of calcium ammonium nitrate fertilizer (13.5% NO_3^-N, 13.5 NH_4^+-N, 4% CaO, 1% Mn, YaraBela® CAN™, YARA GmbHand Co. KG, Dülmen, Germany) applied at a rate of 240 kg N ha^{-1}, split to three doses of 80 kg N ha^{-1} each at BBCH 25, BBCH 30/31 and BBCH 50. The plants were harvested at the grain ripening stage (BBCH 92). The environmental conditions during the experiments are shown in Fig. S4.

$^{13}CO_2$labeling during flowering

In order to quantify the C allocation pattern above- and belowground, we conducted $^{13}CO_2$ pulse labeling during late flowering (BBCH 69). Technical challenges associated with the automatic manifold system that was used to measure the ^{13}C-CO_2, did not allow for earlier labelling during early flowering. The plants were labeled with highly enriched 99 atom-% ^{13}C-CO_2 (Campro Scientific GmbH, Berlin, Germany). Custom-made polymethyl methacrylate plant chambers (Fig. S1), constructed by the workshop of Forschungszentrum Jülich were fitted onto the rhizotrons shortly before the labeling. The chamber comprised a 55° triangle-shaped base (opposite of 5 cm × hypotenuse of 6 cm × adjacent 5 cm, wall thickness of 1 cm) with a rubber seal and the plant compartment (height of 60.7 cm, length of 40.7 cm and width of 8.7 cm, wall thickness of 0.35 cm; total volume of 19 240 cm^3). Two fans (252 N. DC axial fan, 12 V, 25 × 25 × 8 mm, EBM-Papst Mulfingen GmbH and

Co. KG, Mulfingen, Germany) were fixed at the top corners of the chamber to ensure thorough air mixing. A rubber seal port at the uppermost side of the chamber was used to inject the $^{13}CO_2$.

Prior to $^{13}CO_2$ pulse labeling, we monitored the assimilation rate of unlabeled CO_2 inside the chamber by applying four injections of 20 ml pure unlabeled CO_2 to reach a mixing ratio of 1400 ppm CO_2 in the chamber. This was done to adjust the timing of the $^{13}CO_2$ injections as well as to accurately estimate the $^{13}CO_2$ assimilation time by the plants without the need to keep the gas exchange analyzer connected to the plant chamber during the labeling. Prior to the pulse labeling, the soil surface was covered with thick gas-impermeable foil to minimize diffusion of $^{13}CO_2$ into the soil. Air temperature, relative humidity, and mixing ratio of unlabeled CO_2 was monitored with an infrared gas exchange analyzer (Li-8100, Li-COR, Lincoln, NE, USA). When the plants had assimilated most of the CO_2 and its concentration had dropped to sub-ambient levels, another injection was made to reach a CO_2 mixing ratio of 1500 ppm inside the chamber. We repeated this procedure for a different set of environmental factors (temperature range: 25.5–29.5 °C, relative humidity range: 34–50%, light intensity range: 243–618 µmol m^{-2} s^{-1}) to obtain accurate information on how the assimilation rate of the unlabeled CO_2 would change with changes in abiotic conditions. For $^{13}CO_2$ labeling, we made four injections of 20 ml of $^{13}CO_2$ (99 atom % ^{13}C) each in 20-min intervals to ensure that adequate amounts of ^{13}C were fixed by the plants.

In order to facilitate the online isotopic measurements, an automatic valve-switching unit was constructed (Fig. S2) following the setup of Rothfuss et al. (2013, 2015). The time course of soil $\delta^{13}C$ CO_2 at the six abovementioned depths was monitored with an isotope ratio infrared spectrometer (IRIS, Delta Ray™, Thermo Fisher Scientific, Inc., Waltham, MA, USA) after the $^{13}CO_2$ pulse labeling. Data was recorded 2 h after labeling (0 days after labeling, DAL), for two consecutive days after labeling and on the tenth and twenty-fifth day after labeling (DAL). Every time we fitted the chamber onto the rhizotron, the soil surface was covered with gas-impermeable foil to prevent gas exchange between the soil and the chamber interior. For the online time-series measurement, we contrasted W1 and W4. W2 plants were also labelled on the same day as W1 and W4 but were not used for these online measurements. The $\delta^{13}C$ was measured at harvest in the plant biomass and in various soil pools in all three rotational positions. The excess ^{13}C CO_2 was calculated based on the atom% ^{13}C excess of every sample, its biomass and C content. All calculations were corrected for the background unlabeled ^{13}C, assuming a $\delta^{13}C$ CO_2 of -27‰ of our cereal-dominated soil at the beginning of the experiment. We expressed the excess ^{13}C CO_2 as a flux of mg^{13}C CO_2 min^{-1} by using the flow rate of 100 mL min^{-1} of CO_2-free air that was used in the automatic manifold system and the CO_2 measurements at each soil depth.

Plant harvest and analyses

At harvest (BBCH 92) the aerial plant parts were split into pseudo-stems (hereafter called stems), leaves, husks and grains. The rhizotron plates were removed, and the soil profile was then divided into seven layers (0–10, 10–20, 20–40, 40–50, 50–70, 70–80 and 80–100 cm) and samples from all soil depths were taken. Due to the extensive root growth throughout the rhizotron, there was no root-free bulk soil. Therefore, we considered the soil to be root-affected. Within every soil depth, several soil aliquots were pooled to form a composite sample and then split into several samples before the analysis. The roots were retrieved after washing off the soil through a 1-mm sieve and stored in 30% ethanol. They were scanned on a flatbed scanner (Epson Perfection V800 Photo, Epson, Japan) at 600 dpi to retrieve root growth parameters using the WinRhizo® software (Regent Instruments Inc., Quebec, Canada). All plant material was ball-milled (MM 400, Retsch, Germany) and weighed into tin capsules (HEKAtech, Wegberg, Germany) for determination of ^{13}C content of the various plant parts (roots, stems, leaves, husks and grains) using an elemental analyzer coupled to an isotope-ratio mass spectrometer (EA-IRMS, Flash EA 2000, coupled to Delta V Plus; Thermo Fisher Scientific Inc., Waltham, MA, USA).

$$\delta^{13}C = \frac{R_{sample}}{R_{VPDB}} - 1 \quad (1)$$

Where R is the isotope ratio ($^{13}C/^{12}C$) of the sample (R_{sample}) and of VPDB (Vienna Peedee Belemnite, R_{VPDB} = 0.0111802; Werner and Brand 2001)

respectively. The excess ^{13}C of the total plant biomass was calculated based on the atom% ^{13}C excess of every sample, its biomass and C content. All calculations were corrected for the background unlabeled ^{13}C, using the fourth unlabeled replicate of each rotational position.

The chloroform-fumigation extraction (CFE) method (Wu et al. 1990; Joergensen 1996) was used to estimate C_{mic} and N_{mic}. Ten grams of fresh soil stored at 4 °C were weighed in beakers and placed inside a desiccator. They were incubated with ethanol-free chloroform (80 ml) at room temperature for 24 h. Soil samples were then extracted with 0.01 M $CaCl_2$ and analyzed with a TOC analyzer (TOC-V + ASI-V + TNM, Shimadzu, Japan). Non-fumigated soil samples were extracted with the same protocol. C_{mic} and N_{mic} were estimated as the difference between the extracted C and N from fumigated and non-fumigated soil samples. The correction factors, kEC = 0.45 and kEN = 0.4, were used for the calculation of the extractable part of C_{mic} and N_{mic}. Ten milliliters of extracted fumigated and non-fumigated soil solution were freeze-dried in polypropylene vials and stored in a desiccator until further processing. Then, 120 µl of deionized H_2O were added into every PP vial to solubilize the precipitate. The solution was then pipetted into 5 mm × 9 mm silver capsules and air-dried for 2 days. The capsules were placed into a desiccator connected to a vacuum pump and incubated with 200 ml HCl for 1 day. After that, they were placed onto a heating plate at 40 °C for 3 h and stored in the freezer at -20 °C overnight. They were then freeze-dried again and fitted into 10 mm × 10 mm silver capsules before ^{13}C analysis with the elemental analyzer as described before. These steps were done to measure the $\delta^{13}C$ of DOC and C_{mic}. The C_{mic} $\delta^{13}C$ was calculated according to Werth and Kuzyakov (2008). The excess ^{13}C of DOC and C_{mic} was calculated based on the atom% ^{13}C excess of every sample and its DOC and C_{mic}, respectively. All calculations were corrected for the background (initial) unlabeled ^{13}C DOC and C_{mic} values measured at the start of the experiment.

Regarding the initial soil properties, soil samples were analyzed for mineral N, DOC, and total extractable nitrogen (TN). They were extracted using 0.01 M $CaCl_2$ (soil-to-solution ratio of 1:4 w: v), vortexed, shaken horizontally for 2 h at 200 rpm, centrifuged for 15 min at 690 × g, filtrated through 0.45 µm PP-membrane filters (Ø 25 mm; DISSOLUTION ACCESSORIES, ProSense B.V., Munich, Germany) stored 4 °C and measured on the following day. The pH was measured in the same solution using a glass pH electrode (SenTix® 940, WTW, Xylem Analytics, Weilheim, Germany). Ammonium (NH_4^+) was measured by continuous-flow analysis (Flowsys, Alliance Instruments GmbH, Freilassing, Germany). Nitrate (NO_3^-) and sulfate (SO_4^{2-}) were measured by ion chromatography (Metrohm 850 Professional IC Anion – MCS, Metrohm AG, Herisau, Switzerland). DOC and TN were quantified with a total organic C (TOC) analyzer (TOC-V + ASI-V + TNM, Shimadzu, Japan). Magnesium was with inductively coupled plasma optical emission spectroscopy (ICP-OES, iCAP 7600; Thermo Fisher Scientific Inc., Waltham, MA, USA). The plant-available phosphorus (P_{CAL}) and potassium (K_{CAL}) were measured with ICP-OES (iCAP 6500; Thermo Fisher Scientific Inc., Waltham, MA, USA) after soil extraction with 0.01 M calcium acetate lactate (CAL) instead of $CaCl_2$ and following the same extraction protocol as mentioned before.

Data analysis

Data were checked for normality using the Shapiro-Wilkinson test and for homogeneity of variances using the Levene test. For data not meeting the assumptions of normality the Yeo-Johnson (Yeo and Johnson 2000) and log transformation were applied. The transformation used for a certain variable is mentioned in the respective table that reports the statistical outcome. The factors in the general linear models (GLM) were rotational position (three levels) and soil depth (seven levels). The data on $\delta^{13}C$ of soil respiration measured on five dates was analysed with repeated measures ANOVA. Date (five levels), rotational position (two levels) and soil depth (three levels) were defined as fixed factors. Bonferroni correction was used for multiple comparisons to identify differences between the contrasted factors at $p \leq 0.05$. Data analysis was performed using R and IBM SPSS Statistics for Windows, version 23 (IBM Corp., Armonk, N.Y., USA). Graphs were made with 'ggplot2' (Wickham 2016) and visualizations of Spearman rank correlation matrices were made with 'ggstatsplot (Patil 2021), using R Statistical Software (v4.2.1; R Core Team 2022).

Results

Excess ^{13}C fluxes of soil respiration

Online measurement of the pulse-labeled excess ^{13}C of soil respiration at six soil depths revealed different allocation patterns of the freshly assimilated C during flowering of WW (Fig. 1). Translocation of photosynthates to greater soil depths (> 30 cm) peaked at two days after labeling (DAL), with a total of 0.006 mg ^{13}C excess min^{-1} and decreased gradually thereafter until 25 DAL. Rotational position had a strong effect (Table S1) on root-derived ^{13}C fluxes during the measurement period of 25 DAL. During the first three measurement time points, there were no significant differences between the rotational positions (Fig. 1a, b, c). The observations during the last two measurement of 10 DAL and 25 DAL, revealed a strong influence of the rotational position on soil respiration of freshly assimilated C. More specifically, there was 87.2% higher ^{13}C excess of the soil respired CO_2 in W1 compared to W4, with the greater differences been measured in the topsoil layers of 25 cm and 35 cm. Interestingly, the fluxes of ^{13}C-CO_2 were 125% higher in W1 compared to W4 25 DAL. This was evident in both the topsoil (151.7% increase at 25 cm and 160.9% increase at 35 cm) and the subsoil (80.1% increase at 65 cm and 61.9% increase at 85 cm; Fig. 1d, e).

Plant excess ^{13}C and yield

Rotational position strongly affected (Table S2) the allocation of freshly fixed C in WW biomass with a significant increase in absolute excess ^{13}C in W1 compared to W2 and W4 (Fig. 2). C allocation also strongly varied between plant parts, with 11.1 mg excess ^{13}C measured in leaves, followed by grains (5.7 mg), stems (5.5 mg), husks (3.3 mg) and roots (0.3 mg). Pairwise comparisons between the rotational positions for every plant part followed the overall trend of decreased excess ^{13}C in W2 and W4

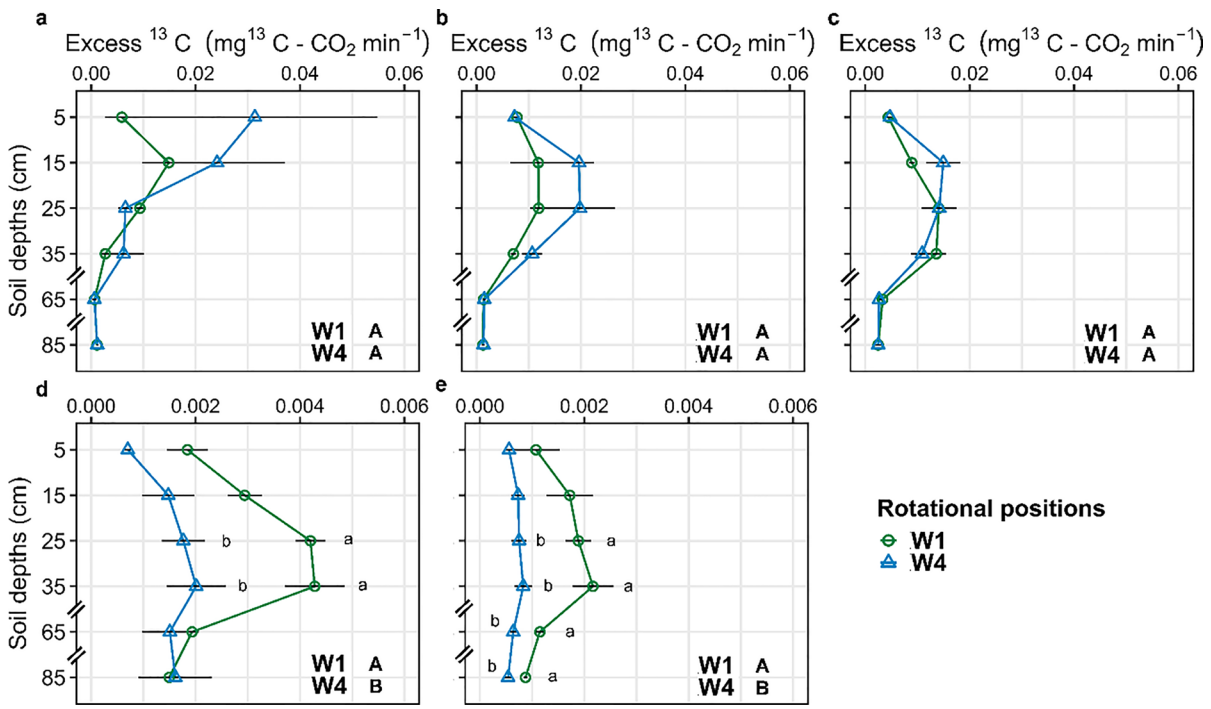

Fig. 1 Excess ^{13}C of soil respiration in two contrasting winter wheat rotational positions 0 (**a**), 1 (**b**), 2 (**c**), 10 (**d**) and 25 (**e**) days after labeling (DAL). Plants were labeled during late flowering (BBCH 69). W1 = first wheat and W4 = fourth wheat after oilseed rape. Different uppercase letters in each subplot indicate significant differences between the rotational positions. Different lowercase letters indicate significant differences between rotational positions at each soil depth at $p \leq 0.05$ level according to repeated measured ANOVA with Bonferroni correction for multiple comparisons

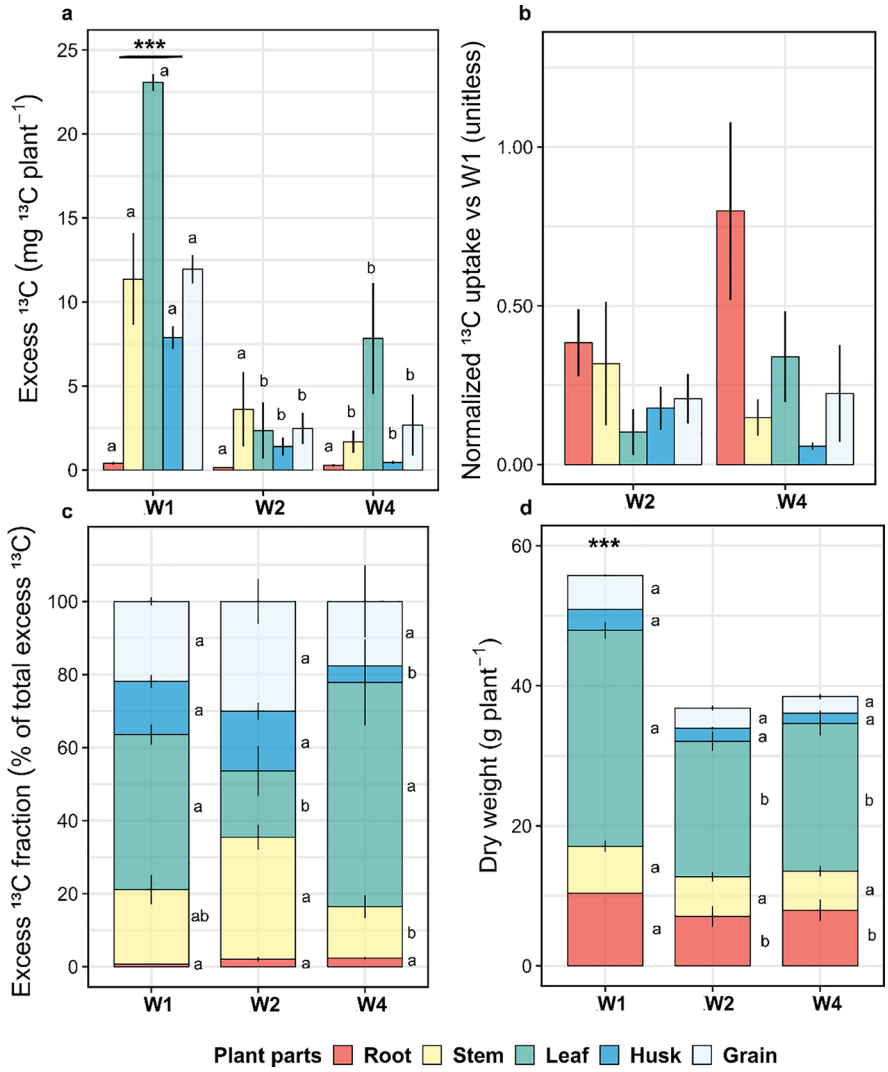

Fig. 2 **a** Absolute excess ^{13}C, (**b**) normalized ^{13}C uptake of W2 and W4 compared to W1, (**c**) relative excess ^{13}C fraction and (d) dry weight of roots, stems, leaves, husks and grains of three rotational positions of winter wheat at grain ripening stage (BBCH 92). W1 = first wheat, W2 = second wheat, and W4 = fourth wheat after oilseed rape. Asterisks indicate significant differences between the rotational positions over all plant parts with $*p \leq 0.05$; $**p \leq 0.01$; $***p \leq 0.001$. Within each plant part, different lowercase letters indicate significant differences between the rotational positions at $p \leq 0.05$ level according to ANOVA with Bonferroni correction for multiple comparisons

compared to W1. More specifically, there was a significant reduction in absolute and normalized excess ^{13}C of W1 compared to W2 and W4 in grain (12.0 mg vs. 2.5 mg and 2.7 mg), husk (7.9 mg vs. 1.4 mg and 0.5 mg) stem (11.4 mg vs. 3.6 mg and 1.7 mg, insignificant for W2) and leaf (23.1 mg vs. 2.4 mg and 7.9 mg) ^{13}C in W1 but not in root ^{13}C (0.4 mg vs. 0.2 mg and 0.3 mg, Fig. 2a, b). W2 plants exhibited a clear shift in their relative allocation of ^{13}C compared to W1 and W4 with lower leaf excess ^{13}C to higher stem excess ^{13}C (Fig. 2c). Finally, the biomass data revealed a similar trend, with 51.5% and 45.0% higher total plant dry weight in W1 compared to W2 and W4, which was mainly due to differences in leaf and root biomass (Fig. 2d).

Excess ^{13}C of belowground pools

Freshly assimilated C was also traced in the microbial biomass (excess ^{13}C C_{mic}), DOC (excess ^{13}C DOC) and root (excess ^{13}C root) pool with decreasing amounts at greater depths (Fig. 3a, b, c; Table S3). Rotational positon had a significant impact on the excess ^{13}C of those three pools (Table S3) with W2 having lower values compared to W1 and W4 overall (Fig. 3a, b, c). Pairwise comparisons revealed a 41.1% reduction in the DOC excess ^{13}C measured in the 10–20 cm of W2 compared to W1 (Fig. 3b). At the same time, there was a 77.1% decrease in the root excess ^{13}C of W2 compared to W1 in the 0–10 cm soil layer (Fig. 3c).

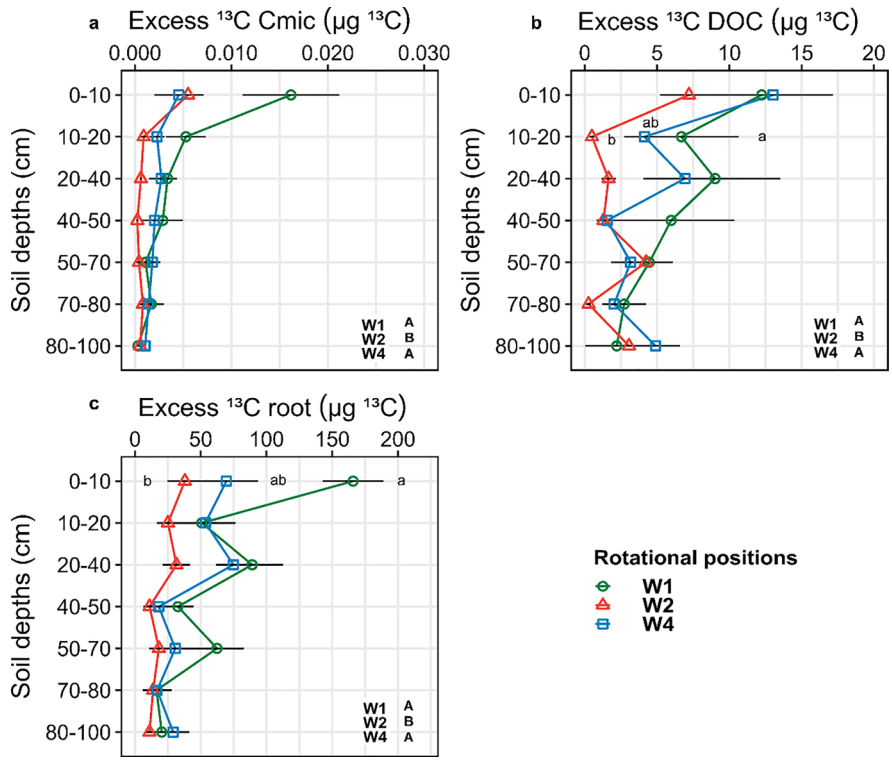

Fig. 3 Absolute excess ^{13}C of the (**a**) microbial biomass C (C_{mic}), (**b**) dissolved organic carbon (DOC) and (**c**) root biomass in three rotational positions of winter wheat at grain ripening stage (BBCH 92). W1 = first wheat, W2 = second wheat, and W4 = fourth wheat after oilseed rape. Different uppercase letters in each subplot indicate significant differences between the rotational positions. Different lowercase letters indicate differences between rotational positions at each soil depth at $p \leq 0.05$ level according to ANOVA with Bonferroni correction for multiple comparisons

The effect of rotational position on root growth

There was a significant main effect of the rotational position on root dry weight (RDW), root mass density (RMD) and root length density (RLD; Table S4; Fig. 4). W1 had a 46.4% and 44.2% higher RDW as well as a 49.9% and 51.1% higher RMD compared to W2 and W4. For RDW, the difference was evident in the 0–10 cm and 20–40 cm (Fig. 4a) while for RMD, it was evident only in the 20–40 cm (Fig. 4b). W1 showed an 36.8% increase in RLD compared to W2 which was mainly due to differences in both top soil (0–10 cm) and subsoil (40–70 cm and 70–100 cm; Fig. 4c). The RLD of W4 did not differ significantly from W1 and was overall 16.1% lower than W1. There was an indication of lower RLD in the 40–70 cm and 70–100 cm of W4; however, this trend was also insignificant.

Rotational position-specific correlation analysis

Correlation analysis (Fig. S5) of the response variables, for each rotational positon, revealed a significant positive correlation between the absolute excess ^{13}C of the root, DOC and C_{mic} in W1.The absolute excess ^{13}C of plant biomass was negatively correlated with RDW and RMD in W1, but positively correlated in W2 and W4. The RLD was positively correlated with plant biomass in W1, but not in W2 and W4. Finally, the RLD of W2 and W4 was negatively correlated with the absolute excess ^{13}C of plant biomass while there was no significant correlation in W1.

Discussion

Using a novel experimental approach, employing real-time quantification of root-derived ^{13}C from $^{13}CO_2$ pulse labeling, we showed that preceding crop legacy is a strong determinant of the above and belowground C allocation in WW. To our knowledge, this is the first time that such non-destructive and real-time method is used to track the fate of photosynthesized C and understand the soil legacy effect of preceding crops to WW.

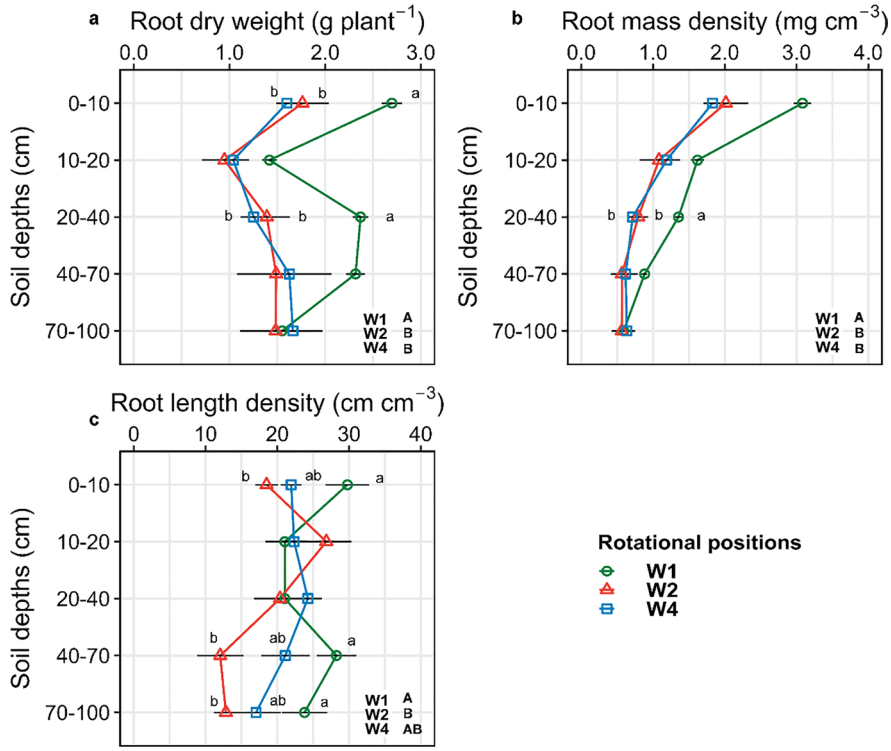

Fig. 4 Root dry weight (**a**), root mass density (**b**) and root length density (**c**) of three rotational positions of winter wheat at grain ripening stage (BBCH 92). W1 = first wheat, W2 = second wheat, and W4 = fourth wheat after oilseed rape. Different uppercase letters in each subplot indicate significant differences between the rotational positions. Different lowercase letters indicate differences between rotational positions at each soil depth at $p \leq 0.05$ level according to ANOVA with Bonferroni correction for multiple comparisons

Winter wheat rotational position strongly influences the translocation of freshly assimilated C belowground

Belowground C allocation is a determinant of several processes, including C and N mineralization rates, residue turnover and microbial community composition (Brüggemann et al. 2011; Pausch and Kuzyakov 2018). Freshly assimilated C has a strong stimulatory effect on rhizosphere processes, including rhizosphere priming and nutrient cycling that are governed by microbial activity (Frey 2019; Wang et al. 2021). C translocation from WW biomass into soil was already evident two hours post $^{13}CO_2$ labeling with high detectable excess ^{13}C fluxes of the soil respiration (Fig. 1). This rapid C translocation to soil has been previously observed in a mountain grassland labeling study assessing diurnal variations in photoassimilate supply to the roots (Bahn et al. 2009). We hypothesized that the soil legacy of successively grown WW will lead to reduced allocation of freshly fixed C due to a negative soil legacy feedback. Initially there was similar excess ^{13}C of the soil respiration in the rhizosphere of W1 and W4. Considering the difference in the initial microbial biomass of W4 and W1 (Table 1), this finding suggests that the microbial community of W1 consumed the rhizodeposits faster than that of W4. The much higher excess ^{13}C of the soil respiration of W1 compared to W4 at 10 and 25 DAL (Fig. 1), provides evidence for accelerated senescence of the root system of W4. Increased belowground C allocation can help plants cope with biotic and abiotic stresses by increasing rhizodeposition and investing more in extensive root systems (Sanders and Arndt, 2012; Chandregowda et al. 2023).

In the soil of successive WW cultivation, the lower excess ^{13}C CO_2 of the soil respiration could be a potential strategy to invest more energy into the production of plant defensive secondary metabolites i.e., benzoxazinones to cope with a less favorable microbial community which can come at the expense of biomass accumulation (Gfeller et al. 2024; Bass 2024). In our experiment, there was no difference in the relative allocation of freshly assimilated C to the root in W2 and W4 compared to W1 suggesting that successive WW (Fig. 2) rotations can not overcome the negative PSF by increasing the translocation of freshly assimilated C to the roots. Reduced rhizodeposition could be also complemented by reduced root growth as both can happen simultaneously (Pausch

and Kuzyakov 2018; Heinemann et al. 2023). This was evident in our study, as shown by the marked decline in RDW, RMD and RLD in successive WW rotation and especially in W2 as well as by the negative correlation between biomass and RLD in the successive WW rotations (Fig. S5). It should be noted that separating autotrophic to heterotrophic respiration is experimentally challenging (Kuzyakov and Larionova 2005).

Uptake of ^{13}C by the rotational position of winter wheat

The excess ^{13}C of the plant biomass of successively grown WW was much lower than that of WW grown after oilseed rape (Fig. 2), which was partially reflected in the lower C translocation belowground (Fig. 1). W1 benefited from the preceding oilseed rape with a higher uptake of ^{13}C compared to self-successional wheat, which was accompanied by a much higher biomass, especially leaf biomass. The aboveground allocation of freshly assimilated C therefore, contributed to the negative PSF in successive WW rotations. The highest amount of excess ^{13}C was measured in the aboveground plant biomass, followed by soil respiration, extractable DOC, and microbial biomass C (C_{mic}). This is consistent with a $^{14}CO_2$ pulse labeling experiment with WW, in which most of the recovered ^{14}C was found in plant biomass and soil respiration, whereas root ^{14}C constituted the smallest pool of the total traced C (Sun et al. 2018). Although we observed relatively low ^{13}C enrichment in the root biomass C pool, we found a higher ^{13}C enrichment of the C_{mic} (Fig. 3), which is opposite to what has been described previously for wheat (Van de Broek et al. 2020) but also other plant species, such as chicory and alfalfa (Hafner and Kuzyakov 2016). For the experiment of Van de Broek et al. (2020), this could relate to the much higher amount of ^{13}C label that entered the system with weekly ^{13}C-pulses as opposed to our single ^{13}C-pulse. However, in another ^{13}C-pulse labeling experiment on maize (Meng et al. 2013), the authors found very low recovery rates for root ^{13}C at grain filling stage compared to elongation phase, while they observed the opposite trend for shoot biomass. This can be attributed to the dynamic C investment strategy of plants that prioritize root elongation during tillering for acquiring nutrients and water over root maintenance, while C translocation to the grain is dominant following anthesis (Sun et al. 2018). Indeed, plants allocated a big portion of the labeled C on aboveground plant parts and especially in the leaves and heads, with lower amounts allocated in the stems and roots. This clearly shows a remobilization and increased translocation of the assimilated ^{13}C towards the reproductive plant organ and thus, the grains of the plants. Thus, the differences in the amount and pattern of ^{13}C allocation between W1 on the one hand, and W2 and W4 on the other hand, suggest a change in the plants' growth strategies depending on the rotational position of WW.

The fate of freshly assimilated C belowground

The amount of ^{13}C traced in the microbial biomass can vary greatly depending on the plant species and variety (Elias et al. 2017; Van de Broek et al. 2020). In addition to autotrophic respiration by the roots, heterotrophic (microbial) respiration substantially contributes to total soil respiration (Brüggemann et al. 2011). In the rhizosphere, heterotrophic respiration is a very important sink of fresh photoassimilates. Similar to other isotopic tracer experiments, we found a strong link between belowground allocation of freshly fixed C and soil respiration, DOC and soil microbial biomass (Bahn et al. 2013; Tavi et al. 2013; Sommer et al. 2016; Weng et al. 2017; Van de Broek et al. 2020). It has been proposed that under conditions of reduced assimilate supply, the lack of carbohydrate reserves in microbes contributes to a faster decline in their respiration rate (Brüggemann et al. 2011). This was not evident in our experiment, as the excess ^{13}C of the soil respiration of W4 was significantly lower compared to W1 during the later growth stage of the plants, while the two rotational positions did not differ in the ^{13}C content of their C_{mic} in the grain ripening stage (Fig. S3). More importantly, we found a higher excess ^{13}C C_{mic} of W1 and W4 compared to W2 (Fig. 3). Both W1 and W4 had higher initial C_{mic} values than W2 at the start of the experiment (Table 1), while there was no significant difference among the rotational positions at the end of the experiment (Fig. S3). This means that the microbial community of W1 and W4 used more freshly assimilated C for growth compared to W2. Previous research has shown the modulating role of the rotational position on microbiome community structure with distinct changes in the relative abundance

of various bacteria and archaeal phyla in successive WW rotations (Giongo et al. 2024; Kaloterakis et al. 2024).

Soil respiration of root-derived ^{13}C in the subsoil was much lower than the topsoil, especially during the first two DAL, while this effect was only partly evident 25 DAL (Fig. 1). This means that the soil microorganisms were not severely C-limited in the subsoil even if there were lower ^{13}C amounts of the excess ^{13}C C_{mic}. Therefore, they must have utilized similar amounts of rhizodeposited C under these non C-limiting conditions. This is similar to what Van de Broek et al. (2020) reported, with the topsoil layers being more enriched in $\delta^{13}C_{Cmic}$ compared to the subsoil, but this trend was not significant. Alternatively, it has been proposed that differences in the C use efficiency of the microbes at the different soil depths could explain the insignificant effect of soil depth on $\delta^{13}C_{mic}$ (Li et al. 2021). We also observed a significant main effect of soil depth on the distribution of the excess ^{13}C DOC (Table S3). This suggests that the ^{13}C pool of DOC was largely influenced by the distribution of root biomass and/or rhizodeposits along the soil profile. In addition, we observed a strong effect of rotational position in the excess ^{13}C DOC. There was more ^{13}C traced in the DOC of W1 compared to W2 in both the top- and subsoil as hypothesized. DOC sources include decomposing C compounds from plant residues and litter as well as root exudates, such as organic acids, amino acids and sugars (Kindler et al. 2011; Panchal et al. 2022). Due to its fast turnover time, DOC is an important pool that encompasses changes in old and new C cycling in the soil, and as such is a major determinant of soil respiration (Brüggemann et al. 2011). Here, we found a strong negative correlation between RLD, excess ^{13}C of the overall plant biomass and specifically of the root biomass (Fig. S5). Increasing RLD to compensate for the negative soil legacy of self-succession comes at the expense of incorporating less freshly assimilated C into biomass, contributing to the negative PSF in W2 and W4.

Conclusion

Overall, our results on the ^{13}C traced in soil respiration, plant biomass, labile C and microbial biomass C after ^{13}C pulse labeling suggest increased incorporation of recently assimilated C into biomass, followed by increased C translocation to the rhizosphere of WW after oilseed rape compared to successively grown WW. More of this translocated C was incorporated into microbial biomass directly through root exudation or indirectly through the heterotrophic utilization of root litter. The findings of our experiment enhance our understanding on the PSF of contrasting WW rotational positions with respect to above- and belowground allocation of freshly assimilated C. The indirect effect of reduced C allocation in successively grown WW likely caused by a negative soil legacy effect, results in reduced root performance and thus potentially lower yield compared to more complex crop rotations with higher C allocation below ground. The increased and sustained C investment in the root system of W1 is overcompensated by higher and longer overall plant vigor, ultimately leading to higher yield.

Acknowledgements The authors acknowledge Henning Kage, Nora Honsdorf and Katharina Pronkow (at the Christian-Albrechts-University of Kiel, CAU) for providing the soil and seed material for the experiment, as well as the technical support of Holger Wissel in the soil and plant C and N analyses. We acknowledge the help of Moritz Harings in setting up the automatic manifold system as well the help of Paulina Alejandra Deseano Diaz for instructions regarding the operation of the isotope ratio infrared spectrometer. The authors also acknowledge the support of Mr. Egmen Ayhan and the workshop IBG-2-5-TAK in constructing the rhizotrons and parts of the automatic manifold system. The authors finally acknowledge the assistance of Mohammad Abujar Shuva in root scanning.

Author contributions NK and NB conceived the study. NB and RR designed the rhizotron prototypes. NK prepared the materials and conducted the experiment. NK and NB designed the automatic manifold system. SLG and YR assisted in setting up and running the isotope ratio infrared spectrometer. NK performed the sample acquisition and sample analyses (plant, biochemical). SK supported the sample analyses. NK and NB interpreted the data and wrote the manuscript. NK and NB prepared the draft. NK, SK, SLG, YR, RR and NB provided constructive feedback and revised the manuscript.

Funding Open Access funding enabled and organized by Projekt DEAL. This work was funded by the German Federal Ministry of Education and Research (BMBF) in the framework of the funding initiative “Rhizo4Bio - Importance of the Rhizosphere for the Bioeconomy”, project “RhizoWheat” (grant number 031B0910B).

Data availability The data will be uploaded to the BonaRes Repository for Soil and Agricultural Research Data.

Declarations

Conflict of interest The authors declare no conflict of interests.

References

Angus JF, Kirkegaard JA, Hunt JR et al (2015) Break crops and rotations for wheat. Crop Pasture Sci 66:523–552. https://doi.org/10.1071/CP14252

Arnhold J, Grunwald D, Braun-Kiewnick A, Koch HJ (2023) Effect of crop rotational position and nitrogen supply on root development and yield formation of winter wheat. Front Plant Sci 14:1265994. https://doi.org/10.3389/fpls.2023.1265994

Bahn M, Lattanzi FA, Hasibeder R et al (2013) Responses of belowground carbon allocation dynamics to extended shading in mountain grassland. New Phytol 198:116–126. https://doi.org/10.1111/nph.12138

Bahn M, Schmitt M, Siegwolf R et al (2009) Does photosynthesis affect grassland soil-respired CO_2 and its carbon isotope composition on a diurnal timescale? New Phytol 182:451–460. https://doi.org/10.1111/j.1469-8137.2008.02755.x

Bass E (2024) Getting to the root of divergent outcomes in the modulation of plant–soil feedbacks by benzoxazinoids. New Phytol 241:2316–2319. https://doi.org/10.1111/nph.19545

Bennett JA, Klironomos J (2019) Mechanisms of plant–soil feedback: interactions among biotic and abiotic drivers. New Phytol 222:91–96. https://doi.org/10.1111/nph.15603

Brisson N, Gate P, Gouache D et al (2010) Why are wheat yields stagnating in Europe? A comprehensive data analysis for France. F Crop Res 119:201–212. https://doi.org/10.1016/j.fcr.2010.07.012

Brüggemann N, Gessler A, Kayler Z et al (2011) Carbon allocation and carbon isotope fluxes in the plant-soil-atmosphere continuum: a review. Biogeosciences 8:3457–3489. https://doi.org/10.5194/bg-8-3457-2011

Calderini DF, Slafer GA (1998) Changes in yield and yield stability in wheat during the 20th century. F Crop Res 57:335–347. https://doi.org/10.1016/S0378-4290(98)00080-X

Chai YN, Schachtman DP (2022) Root exudates impact plant performance under abiotic stress. Trends Plant Sci 27:80–91. https://doi.org/10.1016/j.tplants.2021.08.003

Chandregowda MH, Tjoelker MG, Pendall E et al (2023) Belowground carbon allocation, root trait plasticity, and productivity during drought and warming in a pasture grass. J Exp Bot 74:2127–2145. https://doi.org/10.1093/jxb/erad021

Cheng W, Kuzyakov Y (2005) Root effects on soil organic matter decomposition. In Zobel RW, Wright SF (eds) Roots and Soil Management: Interactions Between Roots and the Soil, pp 119–143. https://doi.org/10.2134/agronmonogr48.c7

Cook RJ (2003) Take-all of wheat. Physiol Mol Plant Pathol 62:73–86. https://doi.org/10.1016/S0885-5765(03)00042-0

Crespo-Herrera LA, Crossa J, Huerta-Espino J et al (2018) Genetic gains for grain yield in cimmyt's semi-arid wheat yield trials grown in suboptimal environments. Crop Sci 58:1890–1898. https://doi.org/10.2135/cropsci2018.01.0017

De Long JR, Heinen R, Heinze J et al (2023) Plant-soil feedback: incorporating untested influential drivers and reconciling terminology. Plant Soil 485:7–43. https://doi.org/10.1007/s11104-023-05908-9

de Vries F, Lau J, Hawkes C, Semchenko M (2023) Plant-soil feedback under drought: does history shape the future? Trends Ecol Evol 38:708–718. https://doi.org/10.1016/j.tree.2023.03.001

Donn S, Kirkegaard JA, Perera G et al (2015) Evolution of bacterial communities in the wheat crop rhizosphere. Environ Microbiol 17:610–621. https://doi.org/10.1111/1462-2920.12452

Elias DMO, Rowe RL, Pereira MG et al (2017) Functional differences in the microbial processing of recent assimilates under two contrasting perennial bioenergy plantations. Soil Biol Biochem 114:248–262. https://doi.org/10.1016/j.soilbio.2017.07.026

Enghiad A, Ufer D, Countryman AM, Thilmany DD (2017) An overview of global wheat market fundamentals in an era of climate concerns. Int J Agron 2017. https://doi.org/10.1155/2017/3931897

Frey SD (2019) Mycorrhizal fungi as mediators of soil organic matter dynamics. Annu Rev Ecol Evol Syst 50:237–259. https://doi.org/10.1146/annurev-ecolsys-110617-062331

Gfeller V, Thoenen L, Erb M (2024) Root-exuded benzoxazinoids can alleviate negative plant–soil feedbacks. New Phytol 241:2575–2588. https://doi.org/10.1111/nph.19401

Giongo A, Arnhold J, Grunwald D et al (2024) Soil depths and microhabitats shape soil and root-associated bacterial and archaeal communities more than crop rotation in wheat. Front Microbiomes 3:1–14. https://doi.org/10.3389/frmbi.2024.1335791

Hafner S, Kuzyakov Y (2016) Carbon input and partitioning in subsoil by chicory and alfalfa. Plant Soil 406:29–42. https://doi.org/10.1007/s11104-016-2855-8

Hansen JC, Schillinger WF, Sullivan TS, Paulitz TC (2019) Soil microbial biomass and fungi reduced with canola introduced into long-term monoculture wheat rotations. Front Microbiol 10:1488. https://doi.org/10.3389/fmicb.2019.01488

Hegewald H, Wensch-Dorendorf M, Sieling K, Christen O (2018) Impacts of break crops and crop rotations on oilseed rape productivity: a review. Eur J Agron 101:63–77. https://doi.org/10.1016/j.eja.2018.08.003

Heinemann H, Hirte J, Seidel F, Don A (2023) Increasing root biomass derived carbon input to agricultural soils by genotype selection – a review. Plant Soil 490:19–30. https://doi.org/10.1007/s11104-023-06068-6

Henneron L, Balesdent J, Alvarez G et al (2022) Bioenergetic control of soil carbon dynamics across depth. Nat Commun 13:7676. https://doi.org/10.1038/s41467-022-34951-w

Hernández-Calderón E, Aviles-Garcia ME, Castulo-Rubio DY et al (2018) Volatile compounds from beneficial or pathogenic bacteria differentially regulate root exudation, transcription of iron transporters, and defense signaling pathways in Sorghum bicolor. Plant Mol Biol 96:291–304. https://doi.org/10.1007/s11103-017-0694-5

Joergensen RG (1996) The fumigation-extraction method to estimate soil microbial biomass: calibration of the kEC value. Soil Biol Biochem 28:25–31. https://doi.org/10.1016/0038-0717(95)00102-6

Jones DL, Nguyen C, Finlay RD (2009) Carbon flow in the rhizosphere: carbon trading at the soil-root interface. Plant Soil 321:5–33. https://doi.org/10.1007/s11104-009-9925-0

Kaloterakis N, Rashtbari M, Razavi BS et al (2024) Preceding crop legacy modulates the early growth of winter wheat by influencing root growth dynamics, rhizosphere processes, and microbial interactions. Soil Biol Biochem 191:109343. https://doi.org/10.1016/j.soilbio.2024.109343

Kindler R, Siemens J, Kaiser K et al (2011) Dissolved carbon leaching from soil is a crucial component of the net ecosystem carbon balance. Glob Chang Biol 17:1167–1185. https://doi.org/10.1111/j.1365-2486.2010.02282.x

Kuzyakov Y, Domanski G (2000) Carbon input by plants into the soil. Rev J Plant Nutr Soil Sci 163:421–431. https://doi.org/10.1002/1522-2624(200008)163:4%3c421::AID-JPLN421%3e3.0.CO;2-R

Kuzyakov Y, Larionova AA (2005) Root and rhizomicrobial respiration: a review of approaches to estimate respiration by autotrophic and heterotrophic organisms in soil. J Plant Nutr Soil Sci 168:503–520. https://doi.org/10.1002/jpln.200421703

Kwak YS, Weller DM (2013) Take-all of wheat and natural disease suppression: a review. Plant Pathol J 29:125–135. https://doi.org/10.5423/PPJ.SI.07.2012.0112

Li J, Pei J, Dijkstra FA et al (2021) Microbial carbon use efficiency, biomass residence time and temperature sensitivity across ecosystems and soil depths. Soil Biol Biochem 154:108117. https://doi.org/10.1016/j.soilbio.2020.108117

Loeppmann S, Forbush K, Cheng W, Pausch J (2019) Subsoil biogeochemical properties induce shifts in carbon allocation pattern and soil C dynamics in wheat. Plant Soil 442:369–383. https://doi.org/10.1007/s11104-019-04204-9

Meier IC, Finzi AC, Phillips RP (2017) Root exudates increase N availability by stimulating microbial turnover of fast-cycling N pools. Soil Biol Biochem 106:119–128. https://doi.org/10.1016/j.soilbio.2016.12.004

Meng F, Dungait JAJ, Zhang X et al (2013) Investigation of photosynthate-C allocation 27 days after ^{13}C-pulse labeling of *Zea mays* L. at different growth stages. Plant Soil 373:755–764. https://doi.org/10.1007/s11104-013-1841-7

Mohan S, Kiran Kumar K, Sutar V et al (2020) Plant root-exudates recruit hyperparasitic bacteria of phytonematodes by altered cuticle aging: implications for biological control strategies. Front Plant Sci 11:763. https://doi.org/10.3389/fpls.2020.00763

Moore FC, Lobell DB (2015) The fingerprint of climate trends on European crop yields. Proc Natl Acad Sci U S A 112:2970–2975. https://doi.org/10.1073/pnas.1409606112

Osborne S-J, McMillan VE, White R, Hammond-Kosack KE (2018) Elite UK Winter wheat cultivars differ in their ability to support the colonization of beneficial root-infecting fungi. J Exp Bot 69:3103–3115. https://doi.org/10.1093/jxb/ery136

Palma-Guerrero J, Chancellor T, Spong J et al (2021) Take-all disease: new insights into an important wheat root pathogen. Trends Plant Sci 26:836–848. https://doi.org/10.1016/j.tplants.2021.02.009

Panchal P, Preece C, Peñuelas J, Giri J (2022) Soil carbon sequestration by root exudates. Trends Plant Sci 27:749–757. https://doi.org/10.1016/j.tplants.2022.04.009

Patil I (2021) Visualizations with statistical details: the 'ggstatsplot' approach. J Open Sour Softw 6:3167. https://doi.org/10.21105/joss.03167

Pausch J, Kuzyakov Y (2018) Carbon input by roots into the soil: quantification of rhizodeposition from root to ecosystem scale. Glob Chang Biol 24:1–12. https://doi.org/10.1111/gcb.13850

Pausch J, Tian J, Riederer M, Kuzyakov Y (2013) Estimation of rhizodeposition at field scale: upscaling of a ^{14}C labeling study. Plant Soil 364:273–285. https://doi.org/10.1007/s11104-012-1363-8

R Core Team (2022) R: a language and environment for statistical computing, v4.2.1. Vienna, Austria: R foundation for Statistical Computing. http://www.r-project.org. Accessed 2/4/2024

Ray DK, Mueller ND, West PC, Foley JA (2013) Yield trends are insufficient to double global crop production by 2050. PLoS ONE 8:6. https://doi.org/10.1371/journal.pone.0066428

Reichel R, Kamau CW, Kumar A et al (2022) Spring barley performance benefits from simultaneous shallow straw incorporation and top dressing as revealed by rhizotrons with resealable sampling ports. Biol Fertil Soils 58:375–388. https://doi.org/10.1007/s00374-022-01624-1

Rothfuss Y, Merz S, Vanderborght J et al (2015) Long-term and high-frequency non-destructive monitoring of water stable isotope profiles in an evaporating soil column.

Hydrol Earth Syst Sci 19:4067–4080. https://doi.org/10.5194/hess-19-4067-2015

Rothfuss Y, Vereecken H, Brüggemann N (2013) Monitoring water stable isotopic composition in soils using gas-permeable tubing and infrared laser absorption spectroscopy. Water Resour Res 49:3747–3755. https://doi.org/10.1002/wrcr.20311

Sanders GJ, Arndt SK (2012) Osmotic adjustment under drought conditions BT- Plant responses to drought stress: from morphological to molecular features. In: Aroca R (ed). Springer Berlin Heidelberg, Berlin, Heidelberg, pp 199–229. https://doi.org/10.1007/978-3-642-32653-0

Schauberger B, Ben-Ari T, Makowski D et al (2018) Yield trends, variability and stagnation analysis of major crops in France over more than a century. Sci Rep 8:16865. https://doi.org/10.1038/s41598-018-35351-1

Senapati N, Halford NG, Semenov MA (2021) Vulnerability of European wheat to extreme heat and drought around flowering under future climate. Environ Res Lett 16:24052. https://doi.org/10.1088/1748-9326/abdcf3

Shewry PR, Hey SJ (2015) The contribution of wheat to human diet and health. Food Energy Secur 4:178–202. https://doi.org/10.1002/FES3.64

Sieling K, Stahl C, Winkelmann C, Christen O (2005) Growth and yield of winter wheat in the first 3 years of a monoculture under varying N fertilization in NW Germany. Eur J Agron 22:71–84. https://doi.org/10.1016/j.eja.2003.12.004

Sommer J, Dippold MA, Flessa H, Kuzyakov Y (2016) Allocation and dynamics of C and N within plant–soil system of ash and beech. J Plant Nutr Soil Sci 179:376–387. https://doi.org/10.1002/jpln.201500384

Sun Z, Chen Q, Han X et al (2018) Allocation of photosynthesized carbon in an intensively farmed winter wheat-soil system as revealed by $^{14}CO_2$ pulse labelling. Sci Rep 8:6–15. https://doi.org/10.1038/s41598-018-21547-y

Sun Z, Wu S, Zhu B et al (2019) Variation of ^{13}C and ^{15}N enrichments in different plant components of labeled winter wheat (*Triticum aestivum* L). PeerJ 7:e7738. https://doi.org/10.7717/peerj.7738

Tavi NM, Martikainen PJ, Lokko K et al (2013) Linking microbial community structure and allocation of plant-derived carbon in an organic agricultural soil using $^{13}CO_2$ pulse-chase labelling combined with ^{13}C-PLFA profiling. Soil Biol Biochem 58:207–215. https://doi.org/10.1016/j.soilbio.2012.11.013

Thakur MP, van der Putten WH, Wilschut RA et al (2021) Plant-Soil Feedbacks and temporal dynamics of plant diversity-productivity relationships. Trends Ecol Evol 36:651–661. https://doi.org/10.1016/j.tree.2021.03.011

Tian J, Dippold M, Pausch J et al (2013) Microbial response to rhizodeposition depending on water regimes in paddy soils. Soil Biol Biochem 65:195–203. https://doi.org/10.1016/j.soilbio.2013.05.021

Van de Broek M, Ghiasi S, Decock C et al (2020) The soil organic carbon stabilization potential of old and new wheat cultivars: a $^{13}CO_2$-labeling study. Biogeosciences 17:2971–2986. https://doi.org/10.5194/bg-17-2971-2020

van der Putten WH, Bardgett RD, Bever JD et al (2013) Plant–soil feedbacks: the past, the present and future challenges. J Ecol 101:265–276. https://doi.org/10.1111/1365-2745.12054

Wang R, Bicharanloo B, Shirvan MB et al (2021) A novel ^{13}C pulse-labelling method to quantify the contribution of rhizodeposits to soil respiration in a grassland exposed to drought and nitrogen addition. New Phytol 230:857–866. https://doi.org/10.1111/nph.17118

Weiser C, Fuß R, Kage H, Flessa H (2017) Do farmers in Germany exploit the potential yield and nitrogen benefits from preceding oilseed rape in winter wheat cultivation? Arch Agron Soil Sci 64:25–37. https://doi.org/10.1080/03650340.2017.1326031

Weng ZH, Van Zwieten L, Singh BP et al (2017) Biochar built soil carbon over a decade by stabilizing rhizodeposits. Nat Clim Chang 7:371–376. https://doi.org/10.1038/nclimate3276

Werner RA, Brand WA (2001) Referencing strategies and techniques in stable isotope ratio analysis. Rapid Commun Mass Spectrom 15:501–519. https://doi.org/10.1002/rcm.258

Werth M, Kuzyakov Y (2008) Root-derived carbon in soil respiration and microbial biomass determined by ^{14}C and ^{13}C. Soil Biol Biochem 40(3):625–637. https://doi.org/10.1016/j.soilbio.2007.09.022

Wickham H (2016) ggplot2: elegant graphics for data analysis. Springer-Verlag New York. https://ggplot2.tidyverse.org. Accessed 2/4/2024

Williams A, de Vries FT (2020) Plant root exudation under drought: implications for ecosystem functioning. New Phytol 225:1899–1905. https://doi.org/10.1111/nph.16223

Wu J, Joergensen RG, Pommerening B et al (1990) Measurement of soil microbial biomass C by fumigation-extraction—an automated procedure. Soil Biol Biochem 22:1167–1169. https://doi.org/10.1016/0038-0717(90)90046-3

Yeo INK, Johnson RA (2000) A new family of power transformations to improve normality or symmetry. Biometrika 87:954–959. https://doi.org/10.1093/biomet/87.4.954

Yin C, Schlatter D, Hagerty C et al (2022) Disease-induced assemblage of the rhizosphere fungal community in successive plantings of wheat. Phytobiomes J 7:100–112. https://doi.org/10.1094/pbiomes-12-22-0101-r

Zadoks JC, Chang TT, Konzak CF (1974) A decimal code for the growth stages of cereals. Weed Res 14:415–421. https://doi.org/10.1111/j.1365-3180.1974.tb01084.x

Zhao G, Sun T, Zhang Z et al (2023) Management of take-all disease caused by *Gaeumannomyces Graminis* var. *Tritici* in wheat through *Bacillus subtilis* strains. Front Microbiol 14:1118176. https://doi.org/10.3389/fmicb.2023.1118176

Zhu P, Burney J, Chang J et al (2022) Warming reduces global agricultural production by decreasing cropping frequency and yields. Nat Clim Chang 12:1016–1023. https://doi.org/10.1038/s41558-022-01492-5